Effect of the Consolidation Degree on the Fracture and Failure Behavior of Self-Reinforced Polypropylene Composites as Assessed by Acoustic Emission

Izer A., Stocchi A., Bárány T., Pettarin V., Bernal C., Czigány T.

Accepted for publication in Polymer Engineering and Science
Published in 2010
DOI: 10.1002/pen.21741

Polymer Engineering & Science

Effect of the consolidation degree on the fracture and failure behavior of self-reinforced polypropylene composites as assessed by acoustic emission

Journal:	*Polymer Engineering & Science*
Manuscript ID:	PES-09-0722.R1
Wiley - Manuscript type:	Research Article
Date Submitted by the Author:	
Complete List of Authors:	Izer, András; Budapest University of Technology and Economics, Department of Polymer Engineering Stocchi, Ariel; INTEMA (University of Mar del Plata and National Research Council), Polymer Division Bárány, Tamás; Budapest University of Technology and Economics, Department of Polymer Engineering Pettarin, Valeria; INTEMA (University of Mar del Plata and National Research Council), Polymer Division Bernal, Celina; University of Buenos Aires, Mechanical Engineering Czigany, Tibor; Budapest University of Technology and Economics, Faculty of Mechanical Engineering, Department of Polymer Engineering
Keywords:	fracture, failure, polyolefins, thermoplastics, structure-property relations

Effect of the consolidation degree on the fracture and failure behavior of self-reinforced polypropylene composites as assessed by acoustic emission

András IZER[1], Ariel STOCCHI[2], Tamás BÁRÁNY[1*], Valeria PETTARIN[2], Celina BERNAL[3] and Tibor CZIGÁNY[1]

1. Department of Polymer Engineering, Budapest University of Technology and Economics, H-1111 Budapest, Műegyetem rkp. 3., Hungary.

2. Polymer Science and Engineering Group, INTEMA (University of Mar del Plata and National Research Council), Department of Materials Engineering, Av. Juan B. Justo 4302, B7608FDQ, Mar del Plata, Argentina.

3. Advanced Materials Group, INTECIN (University of Buenos Aires and National Research Council), Department of Mechanical Engineering, Engineering Faculty, Av. Paseo Colón 850, C1063ACV, Ciudad Autónoma de Bs. As., Argentina.

* Author to whom correspondence should be addressed,

E-mail: barany@pt.bme.hu

Submitted to "Polymer Engineering and Science", Nov, 2009 and in revised version, Feb, 2010

Abstract

In this work the fracture and failure behavior of self-reinforced polypropylene composites (SRPPC) was studied. As reinforcement woven fabric, whereas as matrix materials α and β crystal forms of isotactic polypropylene (PP) homopolymer and random PP copolymer (with ethylene) were used. Composite sheets were produced by a film-stacking method and compression molded for constant holding time and at constant pressure but at different processing temperatures to obtain SRPPC sheets with different consolidation quality. The failure behavior of tensile specimens was assessed by the acoustic emission (AE) technique and the typical failure behavior was deduced for the differently consolidated composites. Both the number of AE events and the shape of the cumulative AE events versus deformation curve depend on the adhesion between phases. Correlations between the dominant failure mechanisms and AE events amplitude for model specimens were established which can be used to monitor the damage growth process in SRPPCs.

Keywords: A. Layered structures; A. Polymer-matrix composites (PMCs); D. Acoustic emission; Consolidation

Introduction

Polypropylene (PP) is a useful commodity polymer widely used in the automotive industry which has a good combination of attractive properties. Nevertheless, it has to be filled and reinforced to compete with engineering plastics. A commonly used practice in industry to improve the properties of PP is the incorporation of glass fibers into the polymer. However, recycling of PP-glass fiber composites is difficult because it is usually accompanied with substantial loss in the properties as a result of fiber attrition during reprocessing [1, 2]. Hence, recycling-friendly thermoplastic composites such as self-reinforced composites seem to be very promising alternatives. In self-reinforced polymer composites (also termed “all-polymer composites” or “homocomposites”), the reinforcement and the matrix have identical chemical structures but different melting temperatures. The great advantage of them is their recyclability (since the components can be reprocessed together) and their excellent fiber/matrix adhesion which is ensured without the help of any coupling agent (the best adhesion can be achieved between identical materials). The different melting temperatures can be obtained by exploiting the possibilities of polymer physics (e.g. hot compaction) [3-7]. The basis of this method is that a thin skin of material on the surface of the constrained fiber melts at a suitable temperature. This melted part forms the continuous matrix material. Another technique is the composition of random PP copolymer/PP homopolymer (coextrusion) [8-15], where the copolymer (matrix) is extruded to a homopolymer fiber (reinforcement). The third usual process is a film-stacking method where components having different melting temperatures are put together, e.g. beta/alpha polymorphs of PP [1, 16-19] or of polyamide (PA6) [20].

In addition, in order to design structural components using these composites, a deep understanding of the material behavior and its failure mechanisms is necessary. To this direction, acoustic emission is a powerful non-destructive technique for real-time monitoring of damage development in materials and structures, which has been used successfully for the identification of the damage mechanisms in composite structures under quasi-static and dynamic-cyclic loading. Acoustic

emission (AE) is defined as the generation of transient elastic waves by the rapid release of energy from localized sources within a material undergoing physical changes (deformation). Upon being subjected to the external load, AE may occur from matrix cracking, interface debonding and fiber fracture in composite materials. It is important to identify the source of emission in order to obtain information about fracture mechanisms of composite materials, and it is possible to forecast their imminent fracture. A major issue in the use of the AE technique is how to discriminate the AE signals due to the different damage mechanisms [21]. Many researchers have already worked in this field [22-33] and the amplitude of acoustic emission events has been widely used as a parameter for characterizing damage accumulation. Barre and Benzeggagh [23] testing glass/PP, have reported that the acoustic signal amplitude varies with the different modes of failure. Kumosa et al. [30] have also used the amplitude of acoustic events from glass/polymer to distinguish between types of damage and they have reported that low amplitude events are associated with matrix cracking and high amplitude events with fiber fracture.

In this study, the damage mechanisms in different self-reinforced polypropylene composites (SRPPCs) based on the polymorphism of PP were investigated by the acoustic emission technique. For matrix different PP foils, whereas for reinforcement a woven fabric – woven from highly stretched split PP yarns – were used. The nominal reinforcement content of SRPPCs was 50 wt.%. Composite sheets having a thickness of 2.5 mm were prepared by a film-stacking method and compression molded at three different temperatures to obtain different consolidation.

Experimental

Materials and their processing

As matrix materials three kinds of PP were used: i) β polymorph of isotactic PP homopolymer (H388F); ii) random PP copolymer (R351F), and iii) β polymorph of the latter. The non-nucleated PPs were provided by TVK Co., (Tiszaújváros, Hungary) having a melt flow index of 8 g/10 min

(at 230°C and 2.16 kg load). The β-nucleation of the PP with the help of calcium salt of suberic acid (Ca-sub) was reported in a previous work [18, 19].

The melting temperature (T_m) values of the prepared matrix films were determined by the DSC technique. These values were originally reported in Ref. [18] and are listed here in Table 1. Note that the T_m of α-PP homopolymer is 164.4ºC.

A woven fabric composed from highly stretched split PP yarns with a nominal weight of 180 g/m^2 was selected as reinforcement (its SEM picture has been published before [19]). It was a product of Stradom S.A. (Czestochowa, Poland). This reinforcement has a melting temperature of T_m=172.4ºC (measured by DSC), and tensile strength 465 ± 32 MPa (measured on a single tape) [19].

Composites preparation

Composite plates with a nominal reinforcement content of 50 wt% (i.e. α-PP fabric) and with a thickness of ca. 2.5 mm were produced using the film-stacking method prior to hot pressing. The layers (8 reinforcing plies between 9 matrix films) were placed on each other in cross-ply arrangement in order to obtain orthotropic composite plates, as explained elsewhere [19]. Three different processing temperatures (at 5, 20, and 35 °C above the related matrix melting temperature) were set. The film-stacked packages were inserted between preheated plates, held between them – without applying pressure – for 30 s, pressed for 90 s at 7 MPa and then cooled down with a cooling rate of 10 °C/min as originally reported in Reference [19]. It is noteworthy that the holding time at processing temperature was kept as short and low, respectively, as possible to prevent shrinkage (relaxation) of the fibers.

Specimens and their testing

Static tensile tests were performed on rectangular specimens of 25 x 250 mm^2 (width x length) using a Zwick Z020 universal testing machine with a crosshead speed of 5 mm/min. In order to obtain information about the failure mode, the acoustic emission (AE) technique (Sensophone AED-40 device with Physical Acoustics Corporation Micro30S sensors) was used in the frequency

range of 100-600 kHz with logarithmic amplifying. The threshold was set to 32 dB to filter out ambient noises, and the reference voltage of the test device was 3 mV. An AE sensor was fixed on the surface in the middle of the specimen. To fix the sensor on the surface, a clip was used in each case (composite specimen, and reinforcement tape). To assist the registration of events, silicon gel was used between specimen surface and microphone. With the AE device amplitudes and cumulative events were recorded. The tests were performed at room temperature, and three specimens were tested in all cases. Quite good reproducibility of AE data was observed for all composites. Therefore, only typical curves are plotted in subsequent figures.

In addition, the interlaminar (peel) strength was determined on rectangular specimens of 25.4x250 mm^2 using a Zwick Z020 universal testing machine according to the ASTM D 3167-97 standard at a crosshead speed of 152 mm/min. Attention was paid to peel off the last two reinforcing+matrix layers of the top of the composite sheets. To initiate the peeling, a small piece of aluminium foil was inserted in between the second woven fabric and the third matrix foils in the assembly prior to hot pressing. By this way the related peel results can be compared accordingly.

Results and discussion

Tensile tests and AE

The tensile force and the cumulative AE events as a function of the deformation for the β-rPP-, α-rPP- and β-PP- based SRPPCs are shown in Figures 1, 2 and 3, respectively, for different processing temperatures (T_m+5, +20 and +35°C – a, b and c for each figures, respectively). In order to compare the cumulative AE events of different failures, the AE events were registered until the maximum force. It can be seen in these figures, that with the increase in the processing temperature, the cumulative events strongly decrease (for instance, the cumulative events for the poorly consolidated α-rPP-based SRPPC produced at $T_{processing}=T_m$+5°C are ca. 4200 – see Figure 2 a; for the material produced at $T_{processing}=T_m$+20°C are ca. 200 – see Figure 2 b; and for the α-rPP-based

SRPPC with the highest quality of consolidation processed at $T_{processing} = T_m+35°C$ are ca. 70 – see Figure 2 c). The trend of cumulative AE events for the differently consolidated composites is in good agreement with previous literature [9].

In addition, the shapes of the cumulative AE events vs. deformation curves are significantly different. At the lowest processing temperature of the α-rPP based composite (Figure 2 a), the AE curve increases continuously, and corresponds to a skew line; at $T_{processing}= T_m+20°C$ the AE curve correlates to a 2^{nd} order curve (Figure 2 b); and at the highest processing temperature, the AE curve corresponds to a unit step (Figure 2 c). Furthermore, for the poorly consolidated composites AE events increase steeply in the first part of the curve which may be attributed to the delamination process. With increasing processing temperature and improving consolidation, delamination becomes less dominant and thereby the first part disappears.

To compare the shapes of the cumulative AE events vs. deformation curves more clearly, the data for two β-PP-based composites with significantly different quality of consolidation are replotted in Figure 4. For the composite with poor consolidation, the shape of the cumulative AE events curve rises steeply at even small deformation, and thereafter increases continuously. In the case of the well consolidated SRPPC (having transcrystalline layer), on the other hand, the shape of the cumulative AE events curve corresponds to a unit step and the beginning of the AE event occurs close to final failure. Therefore, the consolidation quality is well reflected by the course of the AE events in agreement with previous findings on commercially available self-reinforced PP composites [34].

In order to achieve good mechanical properties of the composites, good adhesion between the layers is needed. The adhesion can be well quantified, for example, by determining the interlaminar peel strength. In Table 1 the peel strength values as a function of processing temperature for all three kinds of composite materials are also listed. These results have been originally reported in Reference [19]. It can be observed in this Table, that the peel strength increases monotonically with

increasing consolidation temperature in the whole temperature range. Nevertheless, in the case of the β-PP based SRPPC processed at T_m+35°C, peeling became more difficult (unstable delamination). This is well reflected by the high peel strength value underlying considerable scatter which can be attributed to the partial melting of the reinforcing tapes. To compare the peel behavior with the AE events, it can be seen that for the lowest processing temperature, when the adhesion between the fiber and the matrix is poor, the cumulative AE events are very high. But for higher hot pressing temperature, when the peel strength is high, the cumulative AE events are low.

It can be concluded, that as the adhesion between the matrix material and the reinforcement improves, so decrease the AE events, and they also occur later.

Failure mode vs. AE amplitude

The amplitude distribution histogram of events and the typical failure behavior of the β-rPP-, α-rPP- and β-PP- based SRPPCs are shown in Figures 5, 6 and 7, respectively. It can be seen, that for poor consolidation, when the typical failure mechanisms are fiber-matrix debonding and delamination, the typical AE event amplitude is around 40-50 dB, and maximum 70 dB, and the ratio of the lower AE event amplitude (40-50 dB) is high. In the case of the well consolidated composite, on the other hand, for which the typical failure mechanisms are composite and fiber breakage, higher AE event amplitudes appear (80-90 dB), and the ratio of the lower AE event amplitude (40-50 dB) is lower.

In order to investigate the matrix response to AE, tests were also performed on matrix specimens. However, no acoustic events could be detected during tensile tests of the pure PP matrix. A very low level of acoustic activity has also been previously reported in the literature for unreinforced thermoplastic copolyester [22] and neat polypropylene [31]. Therefore, all AE events detected in composites are expected to be due to fabric or matrix-reinforcement interactions.

To study AE response of the pure fabrics, tensile tests were also performed on 50 mm wide reinforcing fabrics. Figure 8 shows the force and the AE amplitude as a function of the deformation. It can be seen, that at fiber crack (reflected by pop-ins in the force-deformation curve – Figure 8a), high AE amplitudes (between 70-90 dB) were detected. However, there were also many events with

lower amplitudes that can be assigned to the movement of alignment of the tapes of the fabrics (Figure 8b). We can therefore conclude that several of the low amplitude events detected on composites with good consolidation are due to some movement of fabric tapes which induced some points of microscopic debonding.

In order to separate the AE events of the fiber crack from the others, tensile tests of single tapes were also performed with similar gauge length than in the case of the fabric and composite specimens. However, there were also many events with lower amplitude beside the events with higher amplitude. This is due to the fact that the tape has fibrillated under loading due to the highly oriented structure. To prevent this fibrillation, small gauge length (15 mm) was set. The results obtained are shown in Figure 9. It can be observed, that pop-ins have occurred in the force-elongation curve (Figure 9a) and few AE events with the amplitude around 60-75 dB were recorded. Figure 9b shows the AE amplitude distribution histogram of events for a single tape. It can be seen, that all events are over 65 dB, so the events with high amplitude correspond to fiber breakage.

It should be noted that in the case of the composite having good consolidation, the transcrystalline layer which is formed between matrix and reinforcement prevented the fibrillation of single tapes. However, for poorly consolidated composites, the fibrillation can occur, but their acoustic response cannot be separated from other events such as alignment of woven fabric.

Conclusions

The aim of this work was to assess the failure mechanisms of self-reinforced PP composites with different consolidation qualities. The SRPP composites composed of woven fabric from highly stretched split PP yarns as reinforcement and α and β crystal forms of isotactic PP homopolymer and random PP copolymer (with ethylene) as matrix materials; were prepared by film-stacking method followed by compression molding at different temperatures. Based on the results of this investigation, it was concluded that the number of AE events depends on adhesion between phases. As matrix-reinforcement adhesion increases, the number of AE events decreases. Poorly

consolidated composites exhibit near 4200 events, while well consolidated ones exhibited less than 70 acoustic events, two orders of magnitude smaller. Besides, the shape of the cumulative AE events vs. deformation curve also depends on adhesion between phases. As matrix-reinforcement adhesion increases, AE events occur nearer to final failure. Poorly consolidated composites exhibited AE events during the entire solicitation, which could be associated with matrix-reinforcement debonding. For well consolidated composites, on the other hand, AE events associated with fiber breakage of tapes only appeared near final fracture. Correlations were established between the dominant failure mechanisms and AE events amplitude for model specimens. Results revealed that low amplitude events (40-50 dB) are generated by movement of alignment of the tapes of the fabric and fiber-matrix debonding, while high amplitude events (over 65 dB) are associated with fiber breakage. These correlations can be used to monitor the damage growth process in SRPPCs. Results revealed that the AE technique is a viable tool for quantifying the matrix-reinforcement adhesion and identifying the damage mechanisms in self-reinforced PP composites.

Acknowledgements

The authors want to thank the National Research Council of Argentina, ANPCyT of Argentina, the Hungarian-Argentinean Intergovernmental Science and Technology Programme (TéT AR-1/2007) and the Hungarian Scientific Research Fund (OTKA F60505).

References

1. T. Bárány, J. Karger-Kocsis and T. Czigány *Polym. Advan. Technol.*, **17**, 818 (2006).
2. A. Pegoretti *Express Polym. Lett.*, **1**, 710 (2007).
3. P.J. Hine, I.M. Ward, N.D. Jordan, R. Olley and D.C. Bassett *Polymer*, **44**, 1117 (2003).
4. P.J. Hine, I.M. Ward and J. Teckoe *J Mater Sci*, **33**, (1998).
5. I.M. Ward *Plast. Rubber Compos.*, **33**, 189 (2004).
6. I.M. Ward and P.J. Hine *Polymer*, **45**, 1413 (2004).
7. A. Izer and T. Barany *Express Polym. Lett.*, **1**, 790 (2007).
8. B. Alcock, N.O. Cabrera, N.M. Barkoula, J. Loos and T. Peijs *Compos. Pt. A-Appl. Sci. Manuf.*, **37**, 716 (2006).
9. B. Alcock, N.O. Cabrera, N.M. Barkoula, A.B. Spoelstra, J. Loos and T. Peijs *Compos. Pt. A-Appl. Sci. Manuf.*, **38**, 147 (2007).
10. T. Bárány, A. Izer and T. Czigány *Plast. Rubber Compos.*, **35**, 375 (2006).
11. S. Houshyar and R.A. Shanks *Macromol. Mater. Eng.*, **288**, 599 (2003).
12. S. Houshyar, R.A. Shanks and A. Hodzic *Express Polym. Lett.*, **3**, 2 (2009).
13. T. Peijs *Mater Today*, **6**, 30 (2003).
14. T. Abraham, K. Banik and J. Karger-Kocsis *Express Polym. Lett.*, **1**, 519 (2007).
15. K. Banik, T.N. Abraham and J. Karger-Kocsis *Macromol. Mater. Eng.*, **292**, 1280 (2007).
16. T.N. Abraham, S. Siengchin and J. Karger-Kocsis *J Mater Sci*, **43**, 3697 (2008).
17. T.N. Abraham, S.D. Wanjale, T. Bárány and J. Karger-Kocsis *Compos Pt A-Appl Sci Manuf*, **40**, 662 (2009).
18. T. Bárány, A. Izer and J. Karger-Kocsis *Polym Test*, **28**, 176 (2009).
19. A. Izer, T. Bárány and J. Varga *Compos Sci Technol*, 2185 (2009).
20. D. Bhattacharyya, P. Maitrot and S. Fakirov *Express Polym Lett*, **3**, 525 (2009).
21. J. Bohse *Compos Sci Technol*, **60**, 1213 (2000).
22. B.A. Acha, N.E. Marcovich and J. Karger-Kocsis *Plast Rubber Compos*, **35**, 73 (2006).

23. S. Barre and M.L. Benzeggagh *Compos Sci Technol,* **52**, 369 (1994).

24. O.I. Benevolenski, J. Karger-Kocsis, T. Czigány and G. Romhány *Compos Pt A-Appl Sci Manuf,* **34**, 267 (2003).

25. T. Czigány *J Compos Mater,* **38**, 769 (2004).

26. T. Czigány, J. Marosfalvi and J. Karger-Kocsis *Compos Sci Technol,* **60**, 1203 (2000).

27. P.J. de Groot, P.A.M. Wijnen and R.B.F. Janssen *Compos Sci Technol,* **55**, 405 (1995).

28. S. Huguet, N. Godin, R. Gaertner, L. Salmon and D. Villard *Compos Sci Technol,* **62**, 1433 (2002).

29. J. Karger-Kocsis, T. Harmia and T. Czigány *Compos Sci Technol,* **54**, 287 (1995).

30. M. Kumosa, D. Hull and J.N. Price *J Mater Sci,* **22**, 331 (1987).

31. K. Renner, M.S. Yang, J. Móczó, H.J. Choi and B. Pukánszky *Eur Polym J,* **41**, 2520 (2005).

32. G. Romhány and G. Szebényi *Express Polym Lett,* **3**, 145 (2009).

33. N.M. Barkoula, B. Alcock, N.O. Cabrera and T. Peijs *Polym Polym Compos,* **16**, 101 (2008).

34. G. Romhány, T. Bárány, T. Czigány and J. Karger-Kocsis *Polym Advan Technol,* **18**, 90 (2007).

Figures captions

Figure 1 Force and number of events as a function of elongation for β-rPP composites produced at different temperatures. (a) T_m+5°C, (b) T_m+20°C, (c) T_m+35°C.

Figure 2 Force and number of events as a function of elongation for the α-rPP composite produced at different temperatures. (a) T_m+5°C, (b) T_m+20°C, (c) T_m+35°C.

Figure 3 Force and number of events as a function of elongation for the β-PP composite produced at different temperatures: (a) T_m+5°C, (b) T_m+20°C, (c) T_m+35°C.

Figure 4 The shape of the cumulative AE events curves for SRPPCs with different consolidation degrees.

Figure 5 The AE amplitude distribution histogram of events and the typical failure behavior of β-rPP composite consolidated at different temperatures. (a) T_m+5°C, (b) T_m+20°C, (c) T_m+35°C.

Figure 6 The AE amplitude distribution histogram of events and the typical failure behavior of α-rPP composite at: (a) T_m+5°C, (b) T_m+20°C, (c) T_m+35°C.

Figure 7 The AE amplitude distribution histogram of events and the typical failure behavior of β-PP composites consolidated at different temperatures. (a) T_m+5°C, (b) T_m+20°C, (c) T_m+35°C.

Figure 8 AE results of breaking of a fabric. (a) Amplitude and force vs. elongation, (b) amplitude distribution histogram of events.

Figure 9 AE results of tensile test for a single tape. (a) Amplitude and force vs. elongation, (b) amplitude distribution histogram of events.

Legend of tables

Table 1 Melting temperature of the matrices and peel strength values for the SRPPCs processed at different consolidation temperatures.

Designation of matrix	Melting temperature of matrix T_m [°C]	Peel strength of the SRPPC processed at T_m+5°C [N/mm]	Peel strength of the SRPPC processed at T_m+20°C [N/mm]	Peel strength of the SRPPC processed at T_m+35°C [N/mm]
β-PP	151.5	0.2	0.75	2.95
α-rPP	142.5	0.33	0.66	1.73
β-rPP	131.3	0.21	0.54	1.36

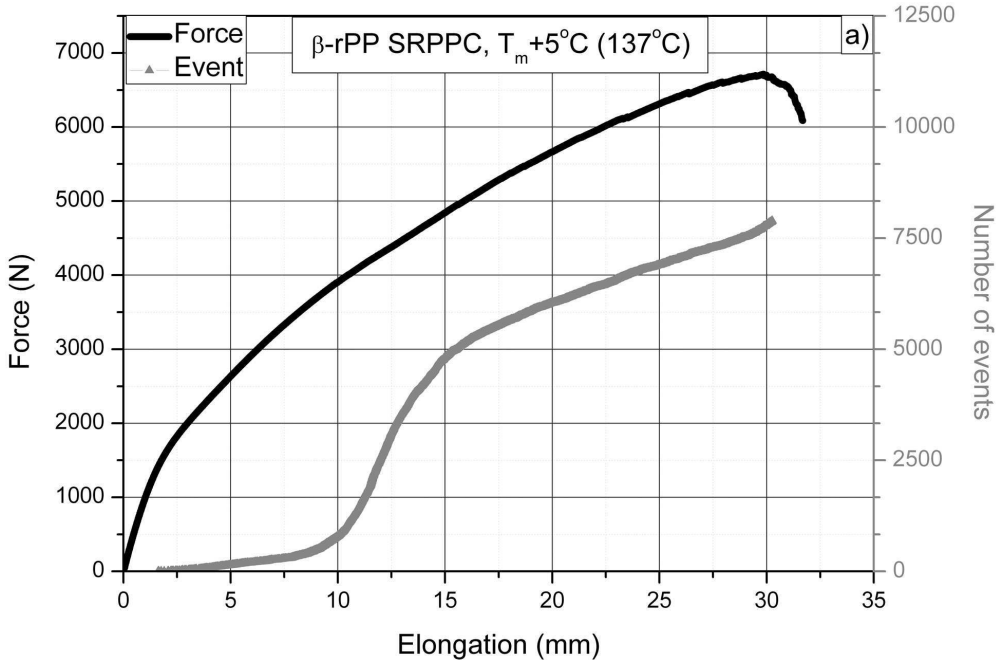

Figure 1 Force and number of events as a function of elongation for β-rPP composites produced at different temperatures. (a) Tm+5°C, (b) Tm+20°C, (c) Tm+35°C
82x54mm (600 x 600 DPI)

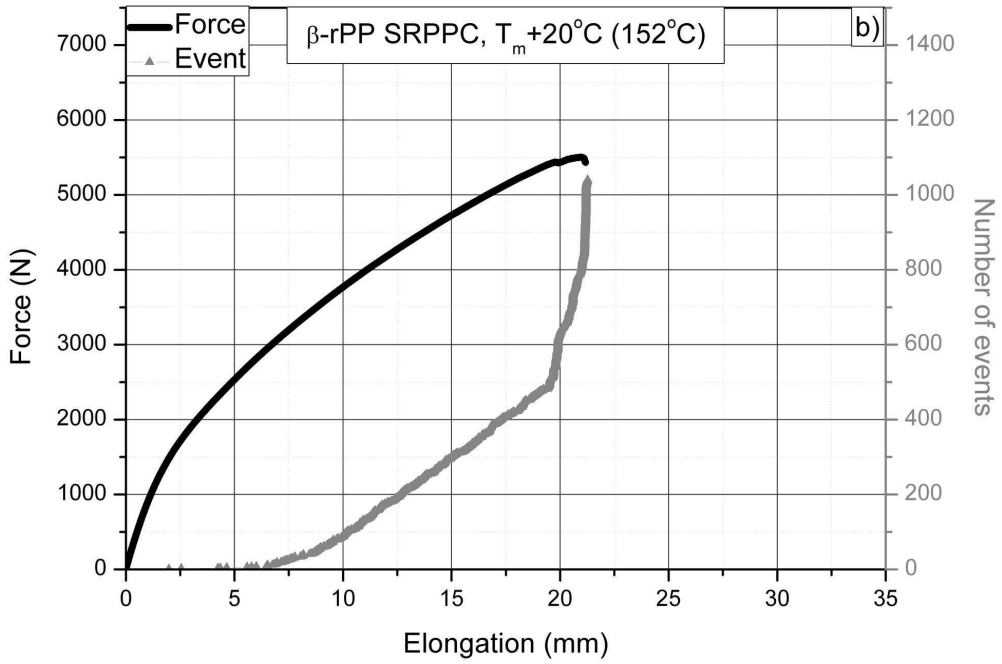

Figure 1 Force and number of events as a function of elongation for β-rPP composites produced at different temperatures. (a) Tm+5°C, (b) Tm+20°C, (c) Tm+35°C
82x54mm (600 x 600 DPI)

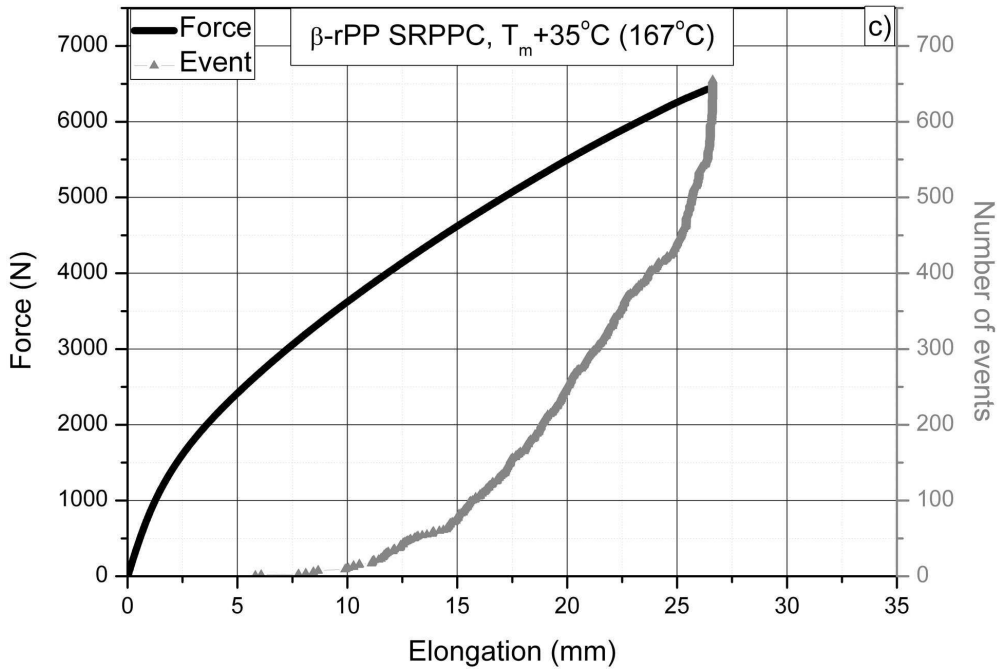

Figure 1 Force and number of events as a function of elongation for β-rPP composites produced at different temperatures. (a) Tm+5°C, (b) Tm+20°C, (c) Tm+35°C
82x54mm (600 x 600 DPI)

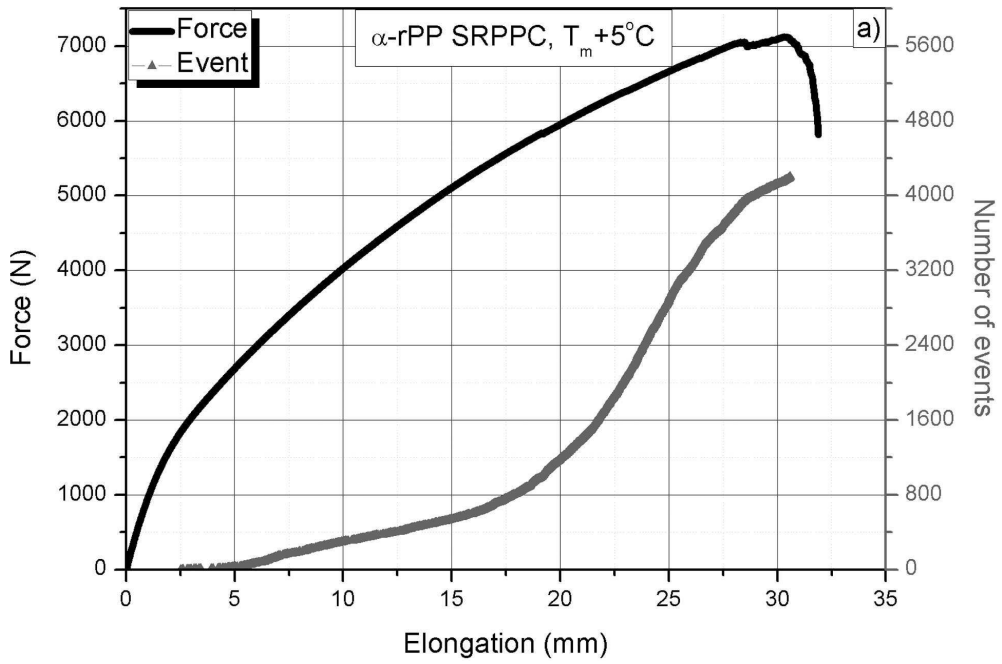

Figure 2 Force and number of events as a function of elongation for the α-rPP composite produced at different temperatures. (a) Tm+5°C, (b) Tm+20°C, (c) Tm+35°C
82x54mm (600 x 600 DPI)

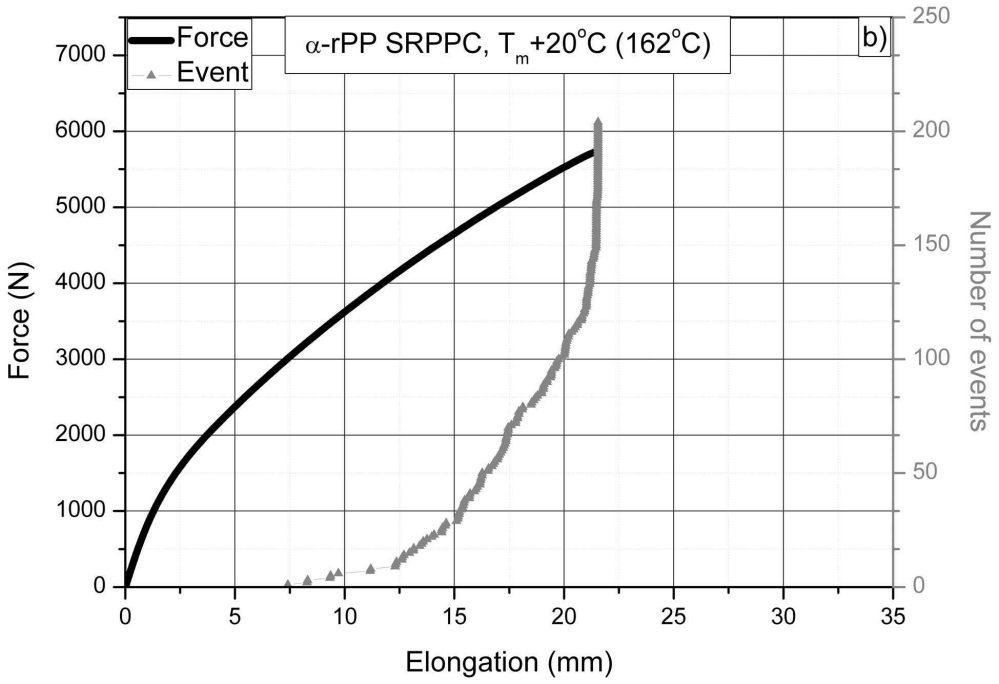

Force and number of events as a function of elongation for the α-rPP composite produced at different temperatures. (a) Tm+5°C, (b) Tm+20°C, (c) Tm+35°C
82x56mm (600 x 600 DPI)

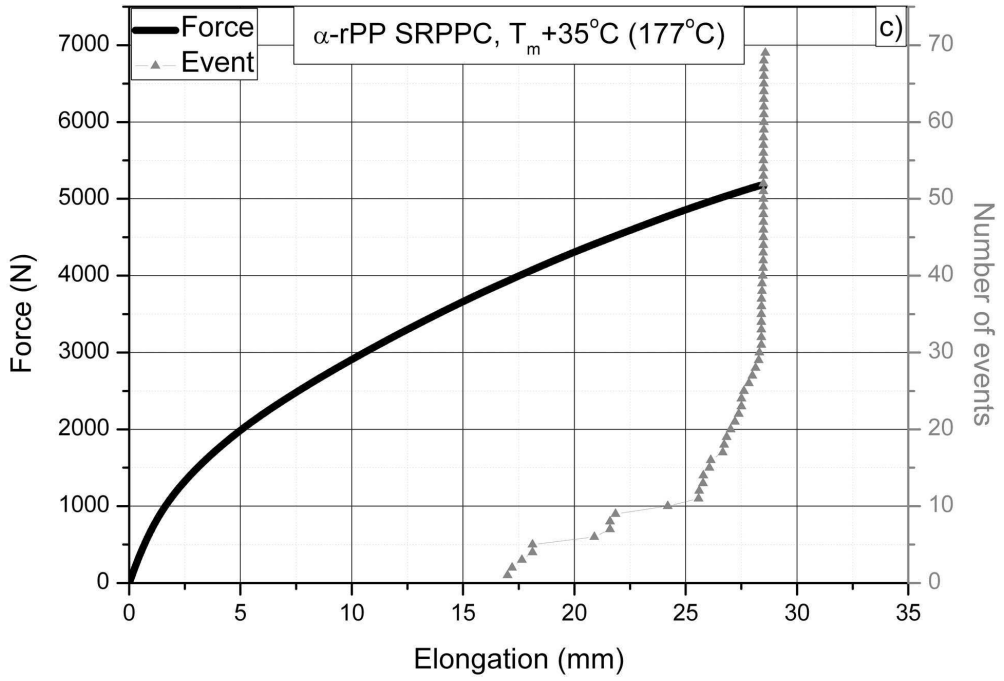

Force and number of events as a function of elongation for the α-rPP composite produced at different temperatures. (a) Tm+5°C, (b) Tm+20°C, (c) Tm+35°C
82x55mm (600 x 600 DPI)

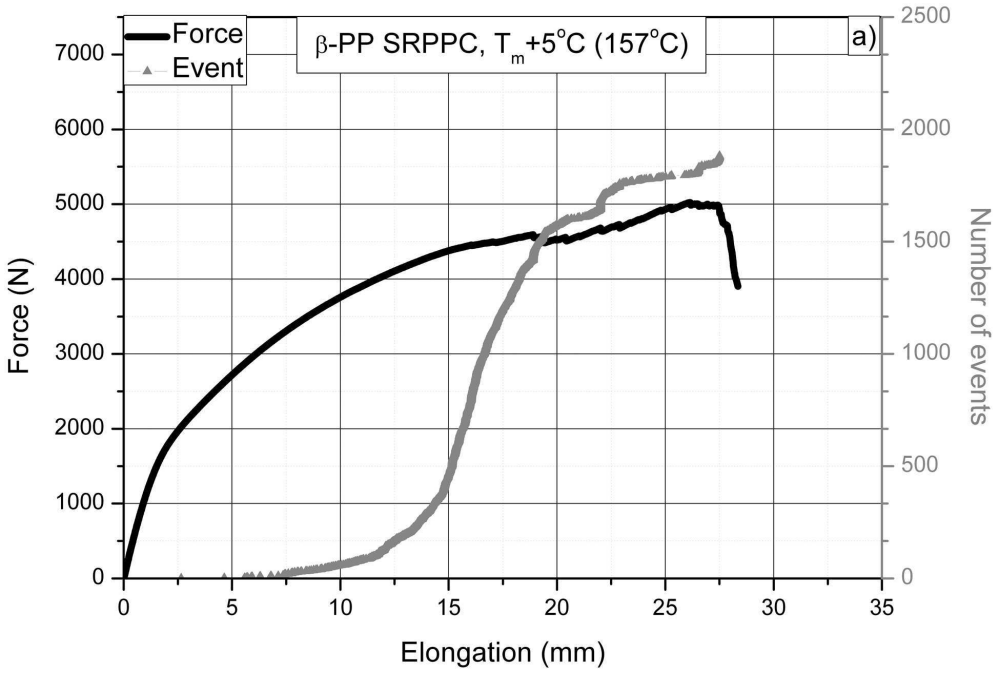

Force and number of events as a function of elongation for the β-PP composite produced at different temperatures: (a) Tm+5°C, (b) Tm+20°C, (c) Tm+35°C
82x55mm (600 x 600 DPI)

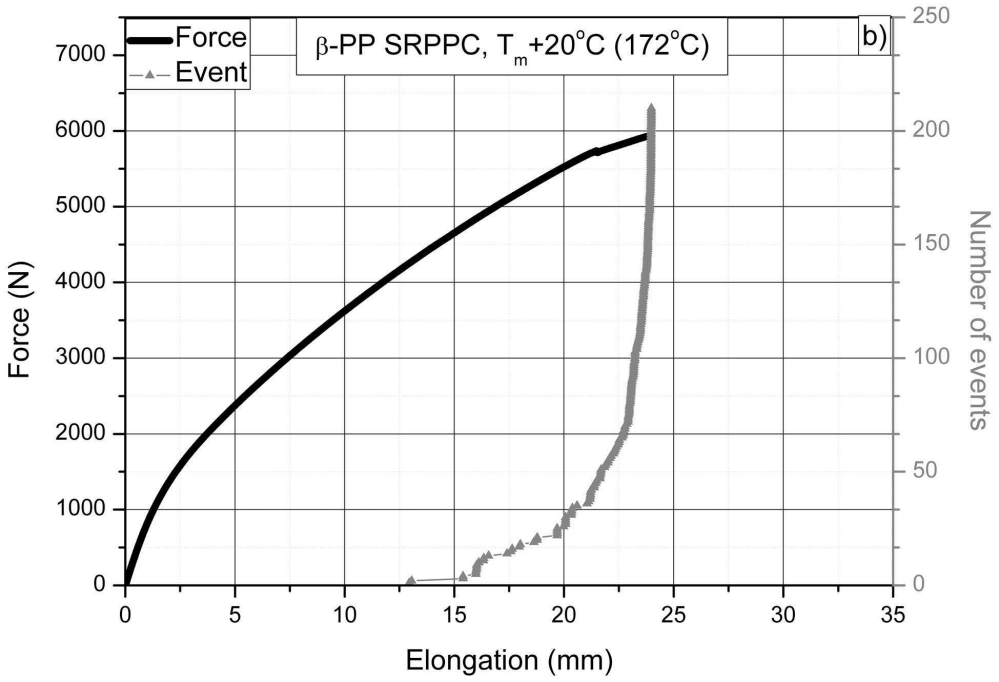

Force and number of events as a function of elongation for the β-PP composite produced at different temperatures: (a) Tm+5°C, (b) Tm+20°C, (c) Tm+35°C
82x56mm (600 x 600 DPI)

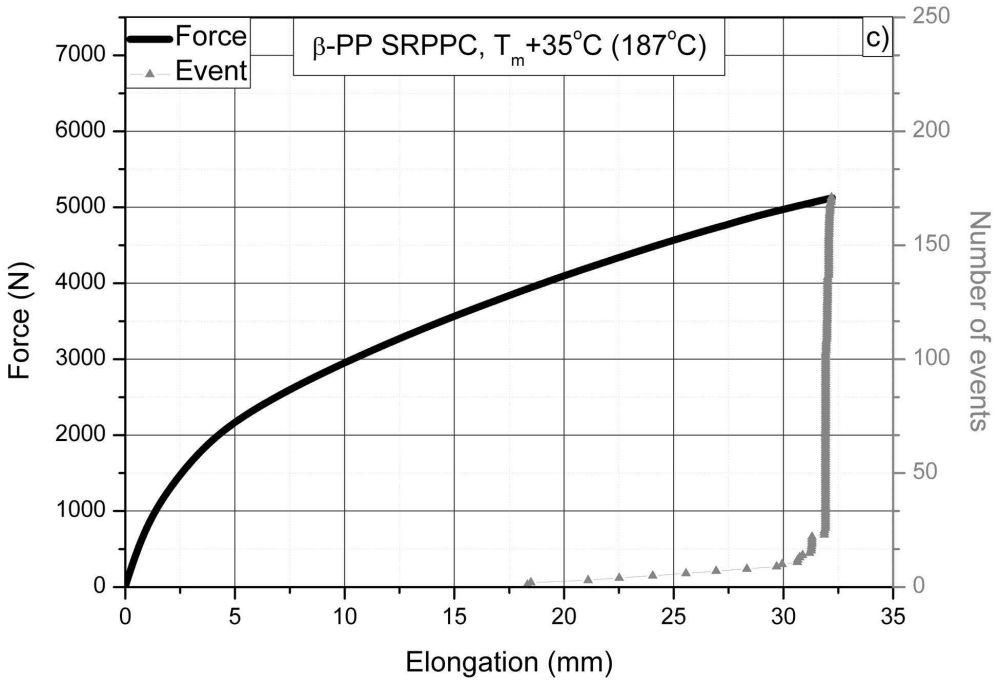

Force and number of events as a function of elongation for the β-PP composite produced at different temperatures: (a) Tm+5°C, (b) Tm+20°C, (c) Tm+35°C
82x56mm (600 x 600 DPI)

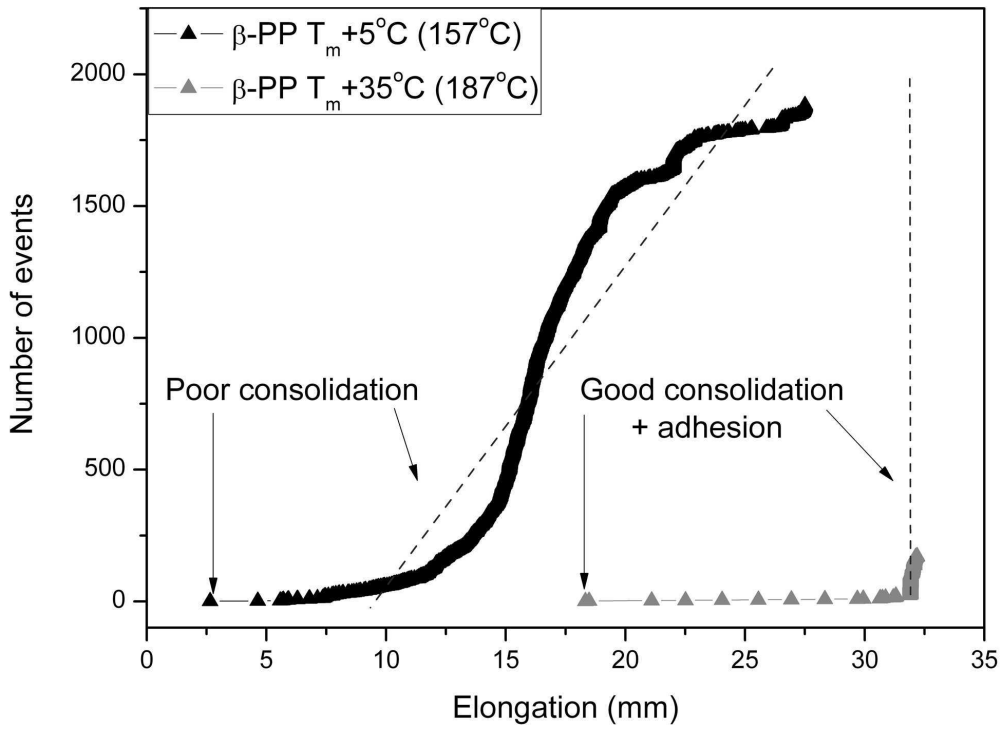

The shape of the cumulative AE events curves for SRPPCs with different consolidation degrees
82x59mm (600 x 600 DPI)

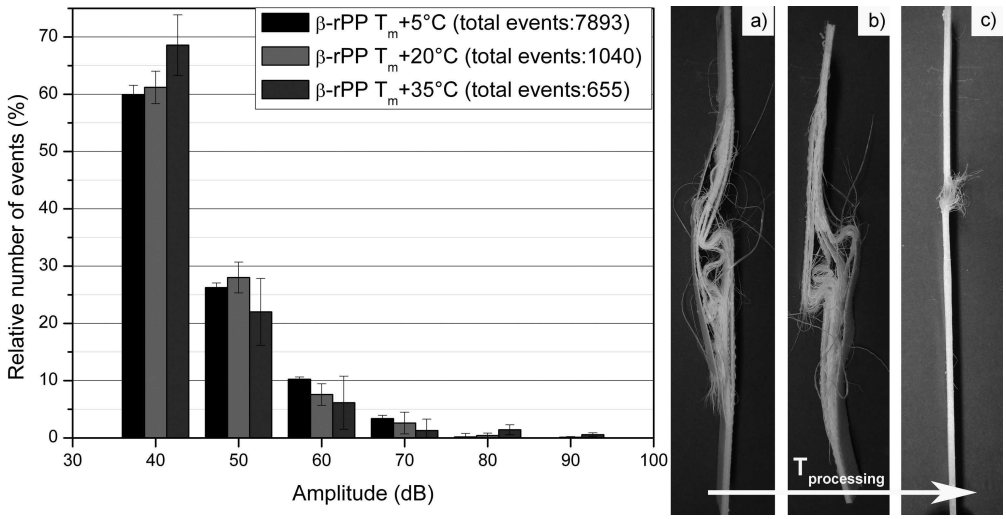

The AE amplitude distribution histogram of events and the typical failure behavior of β-rPP composite consolidated at different temperatures. (a) Tm+5°C, (b) Tm+20°C, (c) Tm+35°C
130x66mm (600 x 600 DPI)

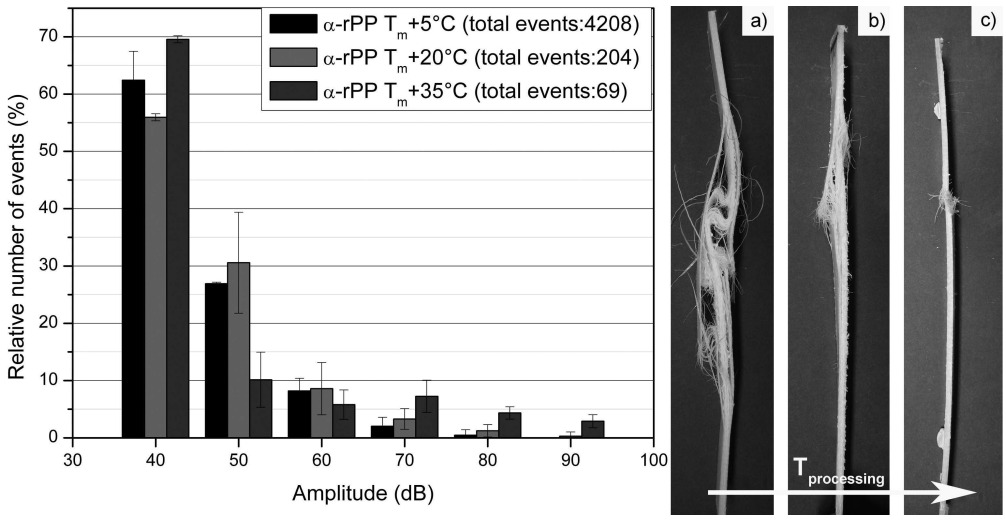

The AE amplitude distribution histogram of events and the typical failure behavior of α-rPP composite at: (a) Tm+5°C, (b) Tm+20°C, (c) Tm+35°C
130x66mm (600 x 600 DPI)

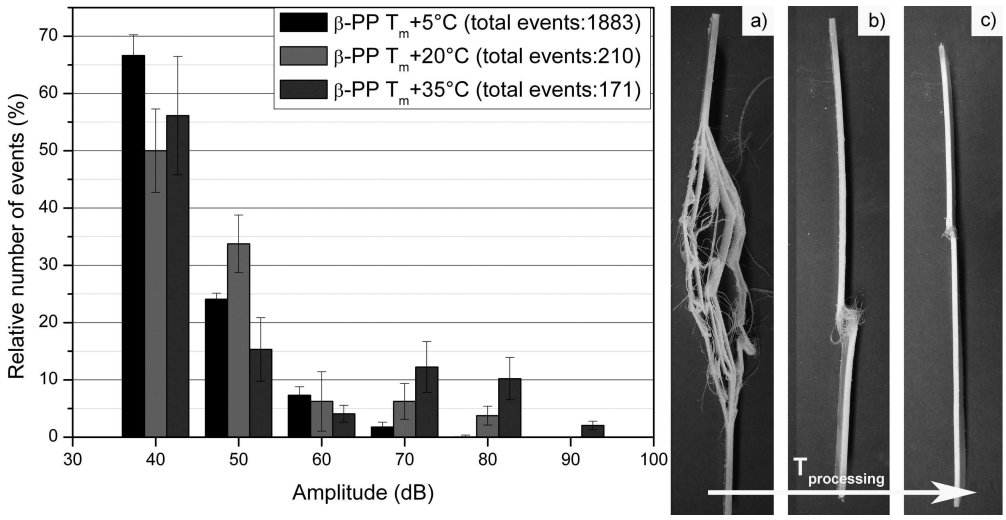

The AE amplitude distribution histogram of events and the typical failure behavior of β-PP composites consolidated at different temperatures. (a) Tm+5°C, (b) Tm+20°C, (c) Tm+35°C
130x66mm (600 x 600 DPI)

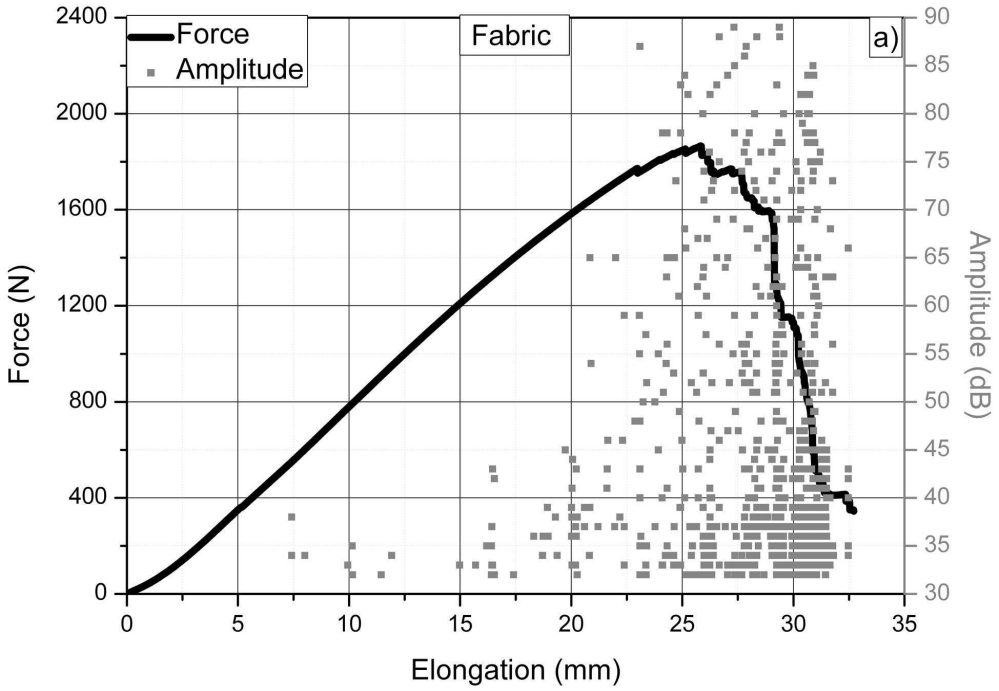

AE results of breaking of a fabric. (a) Amplitude and force vs. elongation, (b) amplitude distribution histogram of events
82x56mm (600 x 600 DPI)

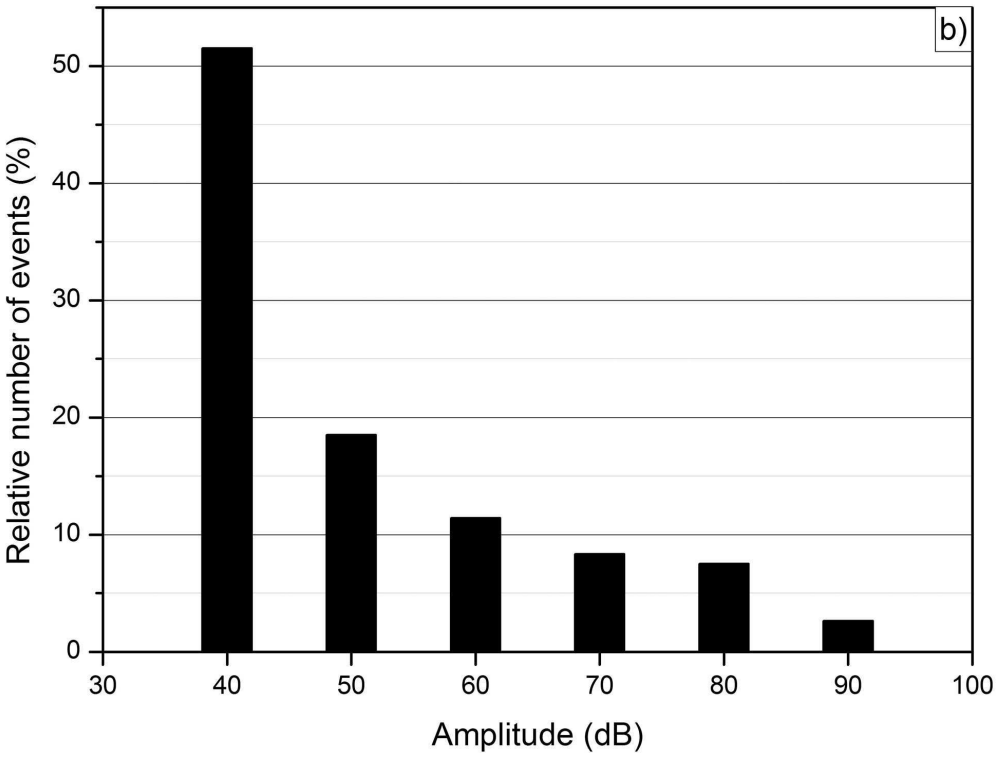

AE results of breaking of a fabric. (a) Amplitude and force vs. elongation, (b) amplitude distribution histogram of events
82x61mm (600 x 600 DPI)

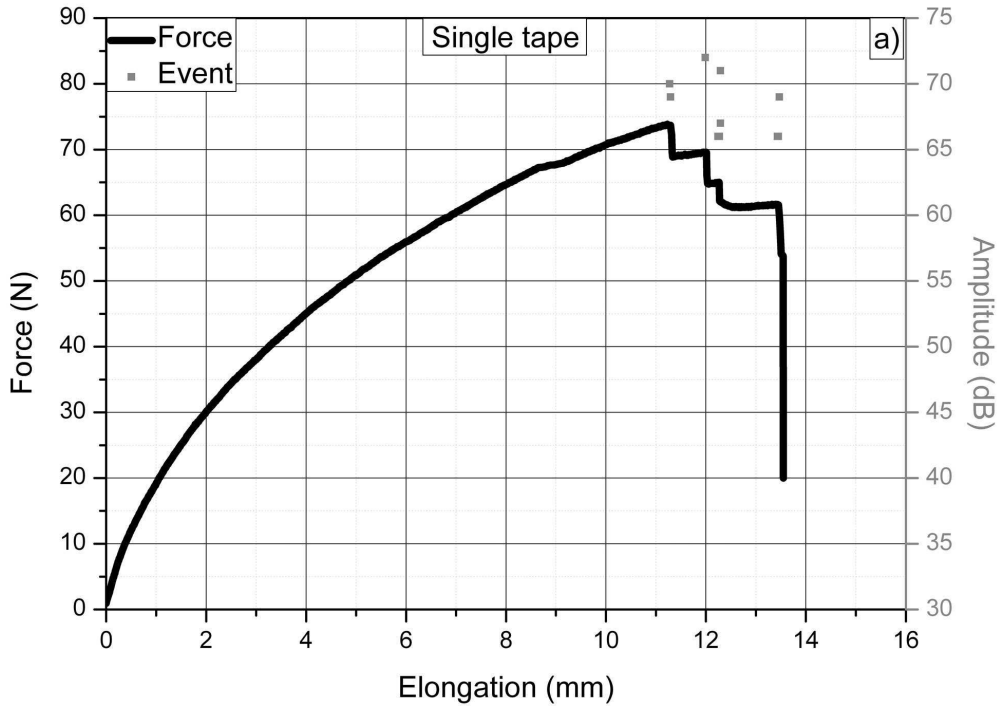

AE results of tensile test for a single tape. (a) Amplitude and force vs. elongation, (b) amplitude distribution histogram of events
82x58mm (600 x 600 DPI)

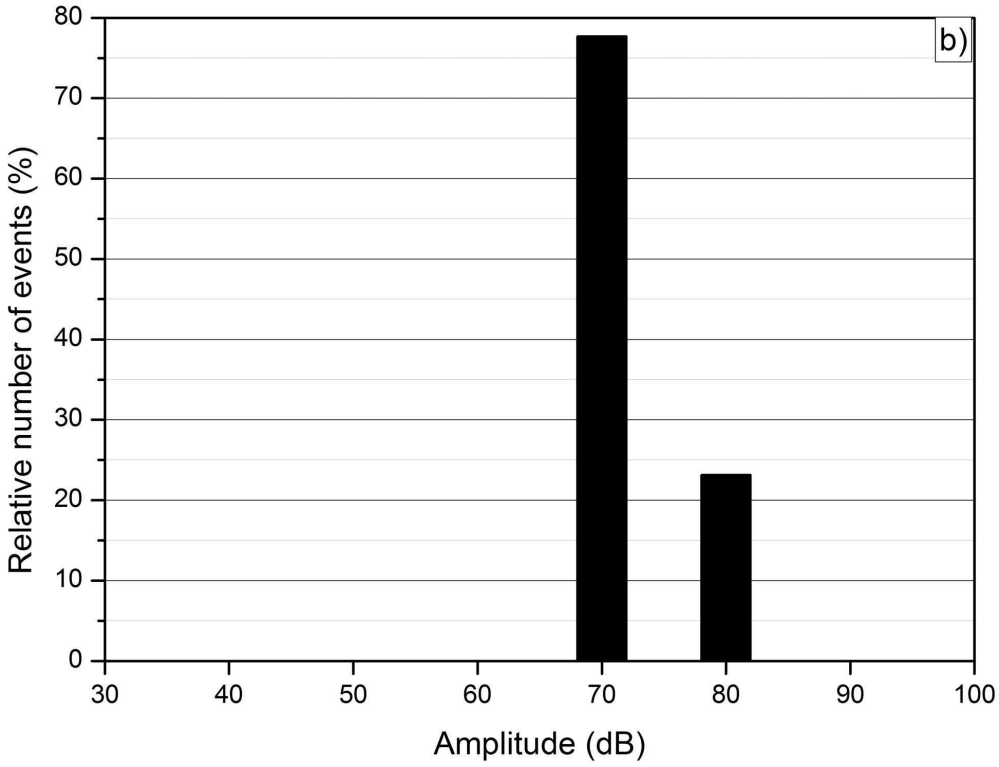

AE results of tensile test for a single tape. (a) Amplitude and force vs. elongation, (b) amplitude distribution histogram of events
82x63mm (600 x 600 DPI)